Imaging of the Carotid Atherosclerotic Plaque with 3T MRI Using dedicated 4-Channel Surface Coils

T. Saam, M.D.; M. F. Reiser, M.D.; K. Nikolaou, M.D.

Dept. of Clinical Radiology, University of Munich, Grosshadern Campus, Munich, Germany

Introduction

Complications of cardiovascular disease, including stroke, myocardial infarction and sudden cardiac death, are the most common cause of death in the world [1]. Atherosclerotic disease accounts for approximately 25% of ischemic strokes and for the majority of myocardial infarctions and sudden cardiac deaths.
Despite major advances in treatment of atherosclerosis, a larger percentage of victims of the disease who are apparently healthy die without prior symptoms [2]. The challenge for screening modalities and diagnostic methods is to identify high risk patients with lesions that are vulnerable to thrombosis, so called "vulnerable plaques", before the event occurs. To tailor and improve treatment strategies, these screening and diagnostic methods must be able to determine the patient-specific risk of suffering a cardiovascular event.
"Vulnerable Plaques" are atherosclerotic plaques which have a high likelihood to cause thrombotic complications, such as myocardial infarction or stroke. Plaques which tend to progress rapidly are also considered to be "vulnerable". Besides luminal stenosis, plaque composition and morphology are key determinants of a plaque's vulnerability to cause cardiovascular events. A classification for clinical as well as pathological evaluation of vulnerable plaques was recently put forward, which proposed 5 major and 5 minor criteria to define vulnerable plaques [3, 4]. These plaque features were based on studies of coronary arteries and included thin caps with large lipid/necrotic core, active inflammation, fissured plaque, stenosis > 90%, endothelial denudation with or without superficial platelet aggregation and fibrin deposition, endothelial dysfunction, calcified nodules, intraplaque hemorrhage, glistening yellow plaques (on angioscopy), and outward remodeling.
Magnetic resonance imaging (MRI) has unique potential to identify the key features of the vulnerable plaque [5]. MRI is well suited for this role because it is non-invasive, does not involve ionizing radiation, enables the visualization of the vessel lumen and wall and can be repeated serially to track progression or regression. Furthermore, recent in vivo MRI studies have shown that MRI allows evaluation of compositional and morphological features of atherosclerotic plaques [6–9]. However, most of this carotid MRI studies were done using 1.5T MRI scanners. Disadvantages of previous carotid MRI studies [6, 10, 11] at 1.5T were relatively long scan times of up to 45 minutes and a relatively high number of excluded subjects due to insufficient image quality in 5–20% of the subjects. Furthermore, the spatial resolution of 0.6 x 0.6 mm (0.3 x 0.3 mm^2 using interpolation techniques) typically used for 1.5T MRI studies might not be able to identify very small features of the atherosclerotic plaque, such as the fibrous cap. This article will give insight into the hardware requirements and MRI protocols currently used at 3T MRI studies, will provide an overview of the literature of recently published 1.5T carotid MRI studies and will discuss the potential role of 3T MRI in identifying the key features of the vulnerable carotid atherosclerotic plaque.

Carotid Surface Coils

MR phased-array surface coil techniques have been used in all vascular beds and have been proven to be effective in improving the signal-to-noise (SNR) ratio in carotid arteries [12]. The carotid arteries are relatively large, superficial and stationary vessels and therefore well suited for high-resolution MR imaging with a phased-array coil assembly consisting of several adjacent small surface coils that collect data simultaneously. Hayes et al. developed a 1.5T MRI phased-array coil for carotid arteries which has an effective longitudinal coverage of up to 5 cm and which improves SNR 37% when compared to a commercially available 3-inch surface coil [12]. The 3T carotid surface coil used at our institution is a dedicated four-channel surface coil (Machnet, Netherlands) which can be used in combination with head and body coils. This allows us to combine the assessment of carotid plaque morphology and composition with an MR angiography of the supraaortal vessels and / or with a brain MRI.

MRI protocol

Thus far, a variety of MRI protocols have been used to assess the carotid wall. While some of the proposed image acquisition techniques rely on one [13] or two [14–16] MR sequences, others are based on multiple contrast-weighted images [6, 17, 18]. The number and type of sequences used depends upon which plaque characteristics are to be studied. For instance, rapid assessment of overall plaque burden is feasible using one or two MR sequences [19, 20]. However, to evaluate plaque composition and morphology in one imaging session, most studies rely on multiple MR sequences. Black-blood T1-, PD- and T2-weighted images with fat and flow suppression enable the visualization of the full vessel wall and are needed to characterize the major plaque components, such as lipid/necrotic core, calcification and loose fibrous matrix [6]. Bright-blood time-of-flight (TOF) images are needed to evaluate the status of the fibrous cap [21, 22] and to identify calcified nodules. Other sequences, such as contrast-enhanced (GD-DPTA) T1-weighted images and dynamic contrast-enhanced 2D spoiled-gradient-recalled-echo-weighted images are useful to quantify lipid/necrotic core size and to evaluate plaque inflammation [23–25]. Furthermore, the use of sophisticated contrast agents, such as USPIOs [26], fibrin [27, 28] – and alpha(v)beta3-integrin [29] – targeted nano-particles offers the promise of in vivo targeted imaging of the plaque.
We currently use a multi-sequence protocol with dynamic contrast enhanced sequences at our 3T MRI scanner which allows to evaluating plaque composition and morphology and provides perfusion data which can be used to assess plaque inflammation in less than 23 minutes (see Table 1, TOF, pre-contrast T1, PD and T2, post-contrast T1 and dynamic contrast enhanced sequences (DCES); best-in-plane resolution 0.5 x 0.5 mm^2 [0.25 x 0.25 mm^2 interpolated]). Parallel imaging is used for all sequences with an acceleration factor (PAT) of 2 for T1-, TOF-, PD and T2-weighted images and a PAT factor of 4 for DCES images. Imaging time for TOF, T1, PD, T2 and DCES images is 4:11, 4:38, 2:08, 2:08 and 5:00 minutes, respectively, resulting in a total scan time of 22:43 minutes.
Fat suppression is used for pre- and post contrast T1W, PDW, and T2W images to reduce signals from subcutaneous and perivascular fat. Each scan covers 30 mm (2 mm thickness x 15 matched images across the 5 sequences). This coverage is usually sufficient to image the complete carotid atherosclerotic plaque.

Table 1: Multi-Sequence 3.0T MRI Protocol

	T1W	PDW	T2W	TOF	DCE*
Sequence	2D-TSE	2D-TSE	2D-TSE	3D-GRE	2D-SR-SGRE
Fat Suppression	Yes	Yes	Yes	Yes	No
TR / ms	800	3000	3000	21	307
TE / ms	12	13	65	3,96	1,72
PAT factor	2	2	2	2	4
ETL	11	13	13	n.a.	n.a.
Flip Angle / °	180	180	180	25	15
Averages	2	2	2	1	3
FOV / mm	160 x 120	160 x 120	160 x 120	160 x 120	160 x 130
Matrix	240 x 320	240 x 320	240 x 320	240 x 320	256 x 208
Number of Slices	15	21	21	52	2
Slice thickness / mm	2	2	2	1	3,5
Pixel size / mm^2 (Interpolated)	0,5 x 0,5 (0,25 x 0,25)	0,5 x 0,5 (0,25 x 0,25)	0,5 x 0,5 (0,25 x 0,25)	0,5 x 0,5 (0,25 x 0,25)	0,625 x 0,625
Scan Time / min	4:38	2:08	2:08	4:11	5:13
Flow Suppression	DIR	Inflow Suppression (Arteries and Veins)	Inflow Suppression (Arteries and Veins)	Inflow Suppression	None

*TI = 159 ms; D = Dimensional; TSE = Turbo Spin Echo; SR-SGRE = Saturation-Recovery

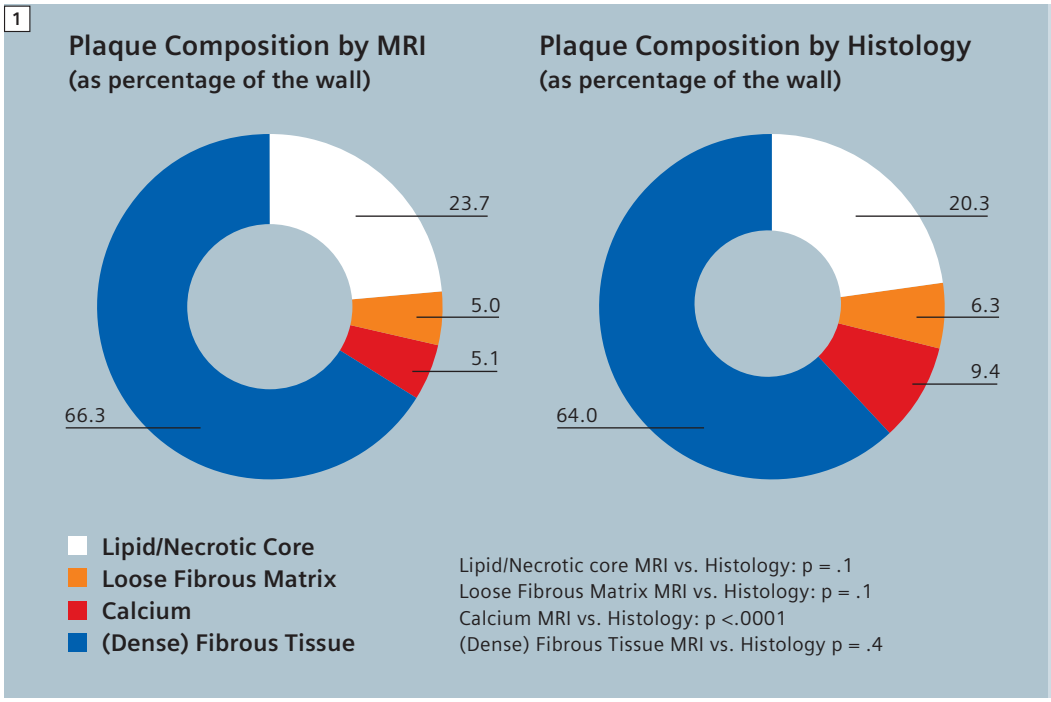

1 This figure shows the plaque composition calculated as percentage of the vessel wall for MRI and histology (the paired t-test was used for statistical comparison. *(With permission of Saam T et al. Arterioscler Thromb Vasc Biol 2005 January; 25(1):234-9)*

MRI validation studies

One of the advantages of carotid in vivo MRI studies is the possibility of histopathological validation using carotid endarterectomy specimen. Several groups have proven [7–9, 13, 30], that in vivo carotid MRI is able to depict all major plaque components, including the lipid/necrotic core, through unique combinations of signal intensity of each component in different contrast weightings. Furthermore MRI is able to quantify the major components of carotid atherosclerotic plaques with good correlation to histology [6]. MRI measurements of plaque composition were statistically equivalent to those of histology (Fig. 1) for the lipid-rich/necrotic core (23.7 vs. 20.3%; p = 0.1), loose fibrous matrix (5.1 vs. 6.3%; p = 0.1) and dense (fibrous) tissue (66.3 vs. 64.0%; p = 0.4). Calcification differed significantly when measured as a percentage of wall area (9.4 vs. 5.0%; p <0.001), but not in absolute area (2.7 vs. 3.5 mm^2; p = 0.1). Other studies have demonstrated that MRI is able to determine the presence, the age and the location of plaque hemorrhages [31–33]. Furthermore, MRI is able to identify the fibrous cap, a layer of connective tissue which is covering the lipid-rich/necrotic core. Lesions with large lipid/necrotic cores and thin, fibrous caps are considered to be most likely to rupture. There are several imaging approaches for MR imaging of the fibrous cap. Hatsukami et al. [21] reported the use of a 3D-TOF bright blood imaging technique (multiple overlapping thin slab angiography, or MOTSA) to identify ruptured fibrous caps in atherosclerotic human carotid arteries in vivo. Trivedi et al. [9] used a short tau inversion-recovery (STIR) to quantify the fibrous cap and lipid/necrotic core of 25 recently symptomatic patients and showed good agreement between MRI and histology. Cai et al. [24] used T1 and contrast-enhanced-T1-weighted images to measure the intact fibrous cap. The authors showed good correlation between carotid MRI and the excised histology specimen for maximal thickness (r = 0.78, p <0.001), length (r = 0.73, p <0.001) and area (r = 0.90, p <0.001) of intact fibrous cap. In our opinion the combination of pre- and post contrast T1, TOF, PD and T2-weighted images has the highest potential to identify the fibrous cap and to differentiate between thick, thin and ruptured fibrous cap. Figures 2A–C show 3T MR images of an intact fibrous cap that is thick (Fig. 2A), an intact but rather thin fibrous cap (Fig. 2B) and a ruptured fibrous cap (Fig. 2C). The differentiation between intact-thick, intact-thin and ruptured fibrous caps is important, as a prospective 1.5T MR study [34] has shown that the presence of a thin or a ruptured fibrous cap at baseline is associated with an increased risk of suffering an ischemic cerebrovascular event during follow-up (hazard ratio, 9.4; 95% CI, 2.1–42.1; P <0.001). The same study found that plaques with intraplaque hemorrhage (hazard ratio, 4.7; 95% CI, 1.6–14.0; P = 0.004), larger maximum % lipid/necrotic core (hazard ratio for 10% increase, 1.4; 95% CI, 1.1–1.9; P = 0.01), and maximum wall thickness (hazard ratio for a 1 mm increase, 1.6; 95% CI, 1.1–2.1; p = 0.007) were associated with occurrence of cerebrovascular events.

1.5T versus 3T MRI

Most imaging of the vessel wall by MRI has been performed at 1.5T scanners. Recently, 3T scanners and their resulting high resolution images have opened the field of vascular imaging to new potentials. These new scanners increase reso-

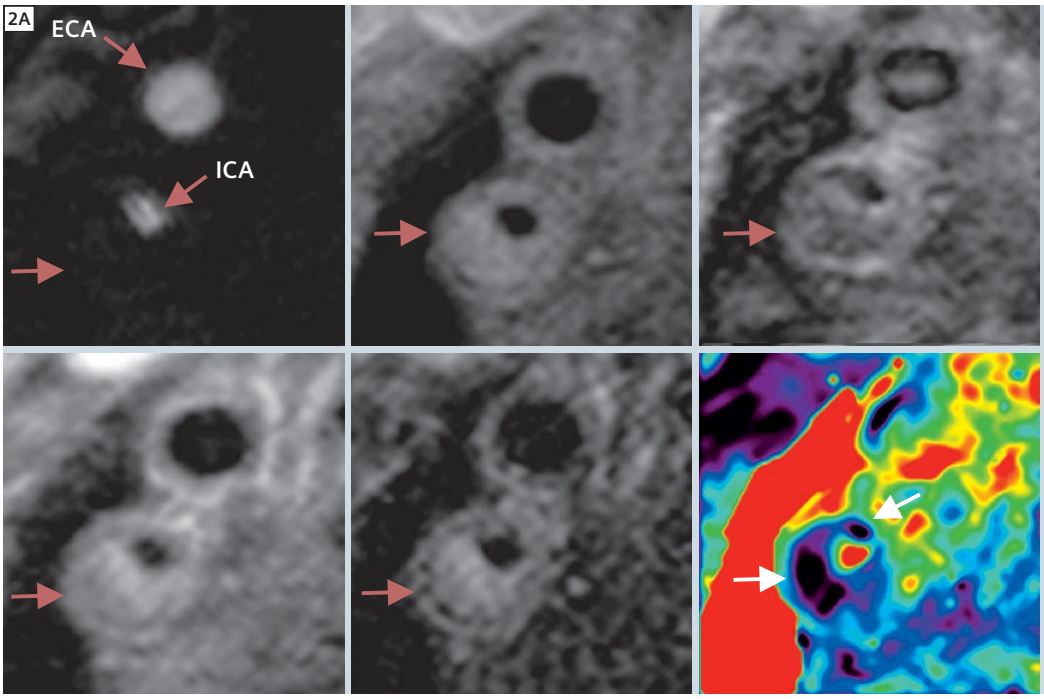

2A Figure 2A shows MR images of a 74-year-old asymptomatic patient with a 90% carotid stenosis in his right internal carotid artery (ICA; ECA = external carotid artery). Cross- sectional MR images show a large eccentric plaque in the right ICA with a large necrotic core without intraplaque hemorrhage (arrow), which is covered by a thick layer of dense and loos fibrous tissue, which can be depicted on T1w-, PD- and T2w- images as a compared to the inner of the plaque moderately hyperintense area near the lumen surface. Extraction flow images show an absence of flow within the lipid/necrotic core (dark area, arrow) and an increased extraction flow in the shoulder of the plaque, indicative of an area of loose fibrous tissue.

lution and image quality. A recent study showed that wall SNR and lumen/wall CNR significantly increased (P < 0.001) at 3T with a 1.5-fold gain for T1-weighted images and a 1.7/1.8-fold gain for PD-/T2-weighted images compared to 1.5T. Quantitative plaque measurements of lumen and wall areas demonstrated good agreement between 1.5 and 3T MRI with no significant bias (P 0.5), a coefficient of variation (CV) of <10%, and intraclass correlation coefficient (ICC) of > 0.95. Another recent study [35] showed signal gains at 3.0T relative to 1.5T for carotid artery wall SNR of 223% and wall-lumen CNR of 255% in all sequences (P <0.025). T1-weighted (T1W) inflow/outflow saturation band (IOSB) and rapid extended coverage double inversion-recovery (REX-DIR) were found to have different levels of SNR and CNR (P <0.05) with IOSB values observed to be larger. While these variations can be resultant of different coil designs, pulse sequences, and contrast weightings, even the most conservative estimates (1.4–1.6 times) provide high potential for improved image resolution and/or shorter scan time. Compared to protocols previously used at 1.5T MRI [36] the protocol which we use at our institution has a larger longitudinal coverage (+ 25%), a smaller pixel size (- 31%) and a shorter scan time, which decreased from 28:30 minutes to 22:43 minutes (17:43 minutes without DCE). Currently the percentage of non-diagnostic scans is approximately 2%, which is substantially smaller than the number of excluded scans in previous 1.5T MRI studies [10, 11], where the number of excluded exams ranged from 5–20%.

A study by Underhill et al. [37] compared the interpretation and quantification of carotid vessel wall morphology and plaque composition at 1.5T with those at 3.0T MRI in 20 subjects with 16%–79% carotid stenosis at duplex ultrasonography. There was a strong level of agreement between field strengths for all morphologic variables, with intra class correlation coefficients ranging from 0.88 to 0.96. Agreement in the identification of presence or absence of plaque components was very good for calcification (kappa = 0.72), lipid/necrotic core (kappa = 0.73), and hemorrhage (kappa = 0.66). However, the visualization of hemorrhage was greater at 1.5T than at 3.0T (14.7% vs. 7.8%, P <.001) and calcifications measured significantly (P = .03) larger at 3.0T. The authors concluded that at higher field strengths, the increased susceptibility of calcification and paramagnetic ferric iron in hemorrhage may alter quantification and/or detection. Nevertheless, imaging criteria at 1.5T for carotid vessel wall interpretation are applicable at 3.0T.

Outlook

Initial experience suggests that imaging of the carotid arterial wall on a 3.0T scanner with dedicated surface coils has a number of advantages, including shorter overall imaging time, higher spatial resolution, larger volume coverage, and improved overall image quality as compared to 1.5T carotid plaque imaging. In our opinion, carotid black-blood multi-echo-sequence 3.0T MRI with parallel imaging is a fast, reproducible and robust method to assess carotid atherosclerotic plaque in vivo. Thus, this method seems to be ready to be used in clinical practice.

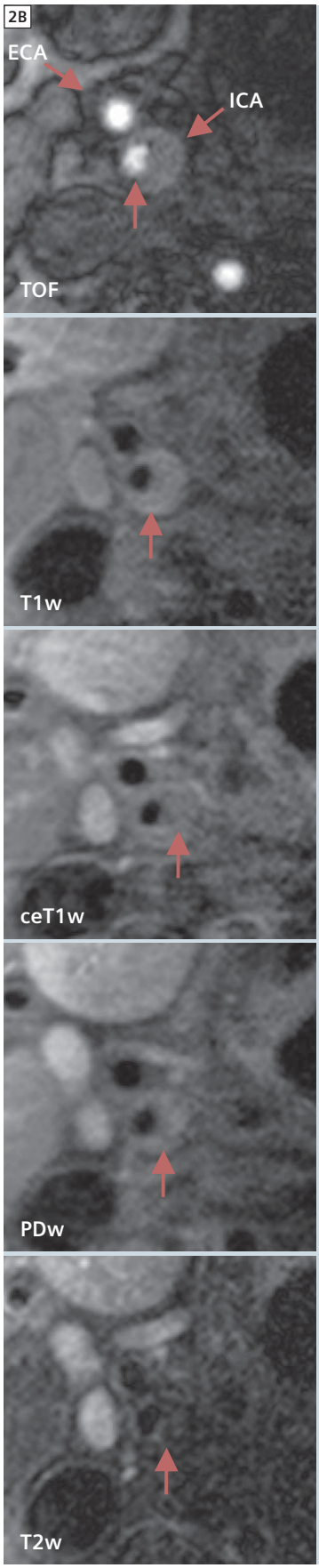

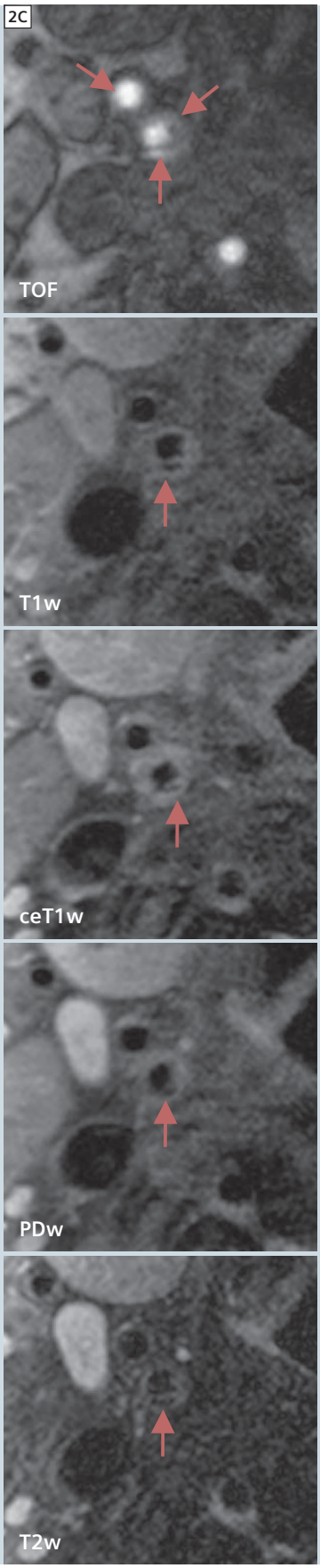

2B, C Figures 2B and C show MR images of the right internal carotid artery of a 78-year-old patient with a right-hemispheric stroke ipsilateral to a 60% carotid stenosis 4 days before the MRI scan.
Figure 2B shows a large eccentric plaque in the left internal carotid artery (ICA) with a large lipid/necrotic core with hemorrhage, which has a high signal intensity on TOF- and pre-contrast T1w images and moderate to low signal intensity on PDw and T2w images and does not enhance on the post contrast T1w images (arrow). The surface of the plaque is smooth, suggesting that the fibrous cap is intact. However, the fibrous cap cannot be differentiated from the lipid/necrotic core and is therefore classified as a thin fibrous cap by MRI criteria.
Figure 2C shows MR images of the same patient 4 mm distally in the ICA. At this location the surface of the plaque appears irregular and TOF images show a very bright area posterior to the lumen of the ICA, corresponding to a hypointense area in all other sequences, suggestive of a ruptured fibrous cap. It is tempting to assume that the rupture of the fibrous cap – which is known to cause thrombotic complications – is the reason for the ischemic stroke in this previously asymptomatic patient.

References

1 World Health Statistics. 2005. Ref Type: Internet Communication.
2 Virmani R, Kolodgie FD, Burke AP, Farb A, Schwartz SM. Lessons from sudden coronary death: a comprehensive morphological classification scheme for atherosclerotic lesions. Arterioscler Thromb Vasc Biol 2000; 20:1262–1275.
3 Naghavi M, Libby P, Falk E, et al. From vulnerable plaque to vulnerable patient: a call for new definitions and risk assessment strategies: Part I. Circulation 2003; 108:1664–1672.
4 Naghavi M, Libby P, Falk E, et al. From vulnerable plaque to vulnerable patient: a call for new definitions and risk assessment strategies: Part II. Circulation 2003; 108:1772–1778.
5 Saam T, Hatsukami TS, Takaya N, et al. The Vulnerable, or High-Risk, Atherosclerotic Plaque: Noninvasive MR Imaging for Characterization and Assessment. Radiology 2007; 244:64–77.
6 Saam T, Ferguson MS, Yarnykh VL, et al. Quantitative evaluation of carotid plaque composition by in vivo MRI. Arterioscler Thromb Vasc Biol 2005; 25:234–239.
7 Toussaint JF, LaMuraglia GM, Southern JF, Fuster V, Kantor HL. Magnetic resonance images lipid, fibrous, calcified, hemorrhagic, and thrombotic components of human atherosclerosis in vivo. Circulation 1996; 94:932–938.
8 Cai JM, Hatsukami TS, Ferguson MS, Small R, Polissar NL, Yuan C. Classification of human carotid atherosclerotic lesions with in vivo multicontrast magnetic resonance imaging. Circulation 2002; 106:1368–1373.
9 Trivedi RA, King-Im J, Graves MJ, et al. Multisequence in vivo MRI can quantify fibrous cap and lipid core components in human carotid atherosclerotic plaques. Eur J Vasc Endovasc Surg 2004; 28:207–213.
10 Saam T, Underhill HR, Chu B, et al. Prevalence of American Heart Association type VI carotid atherosclerotic lesions identified by magnetic resonance imaging for different levels of stenosis as measured by duplex ultrasound. J Am Coll Cardiol 2008; 51:1014–1021.
11 Saam T, Kerwin WS, Chu B, et al. Sample size calculation for clinical trials using magnetic resonance imaging for the quantitative assessment of carotid atherosclerosis. J Cardiovasc Magn Reson 2005; 7:799–808.
12 Hayes CE, Mathis CM, Yuan C. Surface coil phased arrays for high-resolution imaging of the carotid arteries. J Magn Reson Imaging 1996; 6:109–112.
13 Serfaty JM, Chaabane L, Tabib A, Chevallier JM, Briguet A, Douek PC. Atherosclerotic plaques: classification and characterization with T2-weighted high-spatial-resolution MR imaging – an in vitro study. Radiology 2001; 219:403–410.
14 Corti R, Osende JI, Fayad ZA, et al. In vivo noninvasive detection and age definition of arterial thrombus by MRI. J Am Coll Cardiol 2002; 39:1366–1373.
15 Kramer CM, Cerilli LA, Hagspiel K, DiMaria JM, Epstein FH, Kern JA. Magnetic resonance imaging identifies the fibrous cap in atherosclerotic abdominal aortic aneurysm. Circulation 2004; 109:1016–1021.
16 Yonemura A, Momiyama Y, Fayad ZA, et al. Effect of lipid-lowering therapy with atorvastatin on atherosclerotic aortic plaques detected by noninvasive magnetic resonance imaging. J Am Coll Cardiol 2005; 45:733–742.
17 Cappendijk VC, Cleutjens KB, Kessels AG, et al. Assessment of human atherosclerotic carotid plaque components with multisequence MR imaging: initial experience. Radiology 2005; 234:487–492.
18 Clarke SE, Hammond RR, Mitchell JR, Rutt BK. Quantitative assessment of carotid plaque composition using multicontrast MRI and registered histology. Magn Reson Med 2003; 50:1199–1208.
19 Corti R, Fuster V, Fayad ZA, et al. Lipid lowering by simvastatin induces regression of human atherosclerotic lesions: two years' follow-up by high-resolution noninvasive magnetic resonance imaging. Circulation 2002; 106:2884–2887.
20 Lima JA, Desai MY, Steen H, Warren WP, Gautam S, Lai S. Statin-induced cholesterol lowering and plaque regression after 6 months of magnetic resonance imaging-monitored therapy. Circulation 2004; 110:2336–2341.
21 Hatsukami TS, Ross R, Polissar NL, Yuan C. Visualization of fibrous cap thickness and rupture in human atherosclerotic carotid plaque in vivo with high-resolution magnetic resonance imaging. Circulation 2000; 102:959–964.
22 Yuan C, Zhang SX, Polissar NL, et al. Identification of fibrous cap rupture with magnetic resonance imaging is highly associated with recent transient ischemic attack or stroke. Circulation 2002; 105:181–185.
23 Wasserman BA, Smith WI, Trout HH, III, Cannon RO, III, Balaban RS, Arai AE. Carotid artery atherosclerosis: in vivo morphologic characterization with gadolinium-enhanced double-oblique MR imaging initial results. Radiology 2002; 223:566–573.
24 Cai J, Hatsukami TS, Ferguson MS, et al. In vivo quantitative measurement of intact fibrous cap and lipid-rich necrotic core size in atherosclerotic carotid plaque: comparison of high-resolution, contrast-enhanced magnetic resonance imaging and histology. Circulation 2005; 112:3437–3444.
25 Kerwin W, Hooker A, Spilker M, et al. Quantitative magnetic resonance imaging analysis of neovasculature volume in carotid atherosclerotic plaque. Circulation 2003; 107:851–856.
26 Tang T, Howarth SP, Miller SR, et al. Assessment of inflammatory burden contralateral to the symptomatic carotid stenosis using high-resolution ultrasmall, superparamagnetic iron oxide-enhanced MRI. Stroke 2006; 37:2266–2270.
27 Flacke S, Fischer S, Scott MJ, et al. Novel MRI contrast agent for molecular imaging of fibrin: implications for detecting vulnerable plaques. Circulation 2001; 104:1280–1285.
28 Botnar RM, Perez AS, Witte S, et al. In vivo molecular imaging of acute and subacute thrombosis using a fibrin-binding magnetic resonance imaging contrast agent. Circulation 2004; 109:2023–2029.
29 Winter PM, Morawski AM, Caruthers SD, et al. Molecular imaging of angiogenesis in early-stage atherosclerosis with alpha(v)beta3-integrin-targeted nanoparticles. Circulation 2003; 108:2270–2274.
30 Shinnar M, Fallon JT, Wehrli S, et al. The diagnostic accuracy of ex vivo MRI for human atherosclerotic plaque characterization. Arterioscler Thromb Vasc Biol 1999; 19:2756–2761.
31 Chu B, Kampschulte A, Ferguson MS, et al. Hemorrhage in the Atherosclerotic Carotid Plaque: A High-Resolution MRI Study. Stroke 2004; 35:1079–1084.
32 Kampschulte A, Ferguson MS, Kerwin WS, et al. Differentiation of intraplaque versus juxtaluminal hemorrhage/thrombus in advanced human carotid atherosclerotic lesions by in vivo magnetic resonance imaging. Circulation 2004; 110:3239–3244.
33 Cappendijk VC, Cleutjens KB, Heeneman S, et al. In vivo detection of hemorrhage in human atherosclerotic plaques with magnetic resonance imaging. J Magn Reson Imaging 2004; 20:105–110.
34 Takaya N, Yuan C, Chu B, et al. Association Between Carotid Plaque Characteristics and Subsequent Ischemic Cerebrovascular Events: A Prospective Assessment with Magnetic Resonance Imaging – Initial Results. Stroke 2006; In Press.
35 Koktzoglou I, Chung YC, Mani V, et al. Multislice dark-blood carotid artery wall imaging: a 1.5 T and 3.0 T comparison. J Magn Reson Imaging 2006; 23:699–705.
36 Saam T, Hatsukami TS, Yarnykh VL, et al. Reader and platform reproducibility for quantitative assessment of carotid atherosclerotic plaque using 1.5T Siemens, Philips, and General Electric scanners. J Magn Reson Imaging 2007; 26:344–352.
37 Underhill HR, Yarnykh VL, Hatsukami TS, et al. Carotid plaque morphology and composition: initial comparison between 1.5- and 3.0-T magnetic field strengths. Radiology 2008; 248:550–560.

Contact
Tobias Saam, M.D.
Marchioninistr. 15
81377 Munich
Germany
Tel: 0049 (0)89 7095 3520
Fax: 0049 (0) 89 7095 8832
Tobias.Saam@med.uni-muenchen.de